Molecular Dynamics Simulation of Dipalmitoylphosphatidylcholine Membrane with Cholesterol Sulfate

Alexander M. Smondyrev and Max L. Berkowitz
Department of Chemistry, University of North Carolina at Chapel Hill, Chapel Hill, North Carolina 27599 USA

ABSTRACT Using the molecular dynamics simulation technique, we studied the changes occurring in a dipalmitoylphosphatidylcholine (DPPC):cholesterol (CH) membrane at 50 mol% sterol when cholesterol is replaced with cholesterol sulfate (CS). Our simulations were performed at constant pressure and temperature on a nanosecond time scale. We found that 1) the area per DPPC:CS heterodimer is greater than the area of the DPPC:CH heterodimer; 2) CS increases ordering of DPPC acyl chains, but to a lesser extent than CH; 3) the number of hydrogen bonds between DPPC and water is decreased in a CS-containing membrane, but CS forms more water hydrogen bonds than CH; and 4) the membrane dipole potential reverses its sign for a DPPC-CS membrane compared to a DPPC-CH bilayer. We also studied the changes occurring in lipid headgroup conformations and determined the location of CS molecules in the membrane. Our results are in good agreement with the data available from experiments.

INTRODUCTION

Sterol molecules play an important role in biological membranes. Properties of cholesterol (CH)-containing membranes were studied extensively over the last two decades (McMullen and McElhaney, 1996). It was found that inclusion of CH reduces the permeability of membranes, increases molecular order, and produces a condensing effect on membranes. CH also plays a fundamental role in regulating membrane fluidity. Other sterols are also found in various tissues. For example, cholesterol sulfate (CS) is found in spermatozoon plasma membrane (Langlais et al., 1976), stratum corneum (outermost layer of epidermis) (Elias et al., 1984), and erythrocyte membranes (Langlais et al., 1981). The physiological functions of CS are not always exactly known, although it is known to act as a membrane stabilizer; in erythrocyte membranes CS increases protection from osmotic lysis (Bleau et al., 1975), inhibits Sendai virus fusion to erythrocytes (Cheetham et al., 1990), and inhibits the fertilization efficiency of rabbit sperm (Fayrer-Hosken et al., 1987). While CS accounts for only 2% of the total sterol in human sperm, its concentration in the membranes overlying the acrosome is as much as 20%. It is likely that CS contributes to membrane stability in this region (Langlais et al., 1976, 1981). Recent evidence suggests that CS is also involved in epithelial differentiation (Kagehara et al., 1994; Hanley et al., 1997). In human skin CS is synthesized and then hydrolized during the so-called cholesterol sulfate cycle. Loss of intercellular cohesion is associated with the loss of CS during this cycle, while accumulation of CS leads to a thickening of stratum corneum (Wells and Kerr, 1966).

Received for publication 25 June 1999 and in final form 20 December 1999.

Address reprint requests to Dr. Max L. Berkowitz, Department of Chemistry, CB3290, University of North Carolina, Chapel Hill, NC 27599-3290. Tel.: 919-962-1218; Fax: 919-962-2388; E-mail: maxb@unc.edu.

0006-3495/00/04/1672/09 $2.00

Although structures of CH and CS molecules are similar, they have different functions in biological systems. The difference may be due in part to the different polar headgroups in the two molecules. CH has a small polar headgroup—a hydroxyl group. In contrast, CS has a large charged and hydrated polar headgroup (see Fig. 1). Kitson et al. (1992) conducted comparative studies of the effects of CH and CS on properties of palmitoyloleoylphosphatidylethanolamine model membranes. They found that both CH and CS abolish the liquid-crystal to gel transition and produce an ordering effect. However, the ordering effect of CS was weaker compared to that of CH and was attributed to a larger effective area of the lipid:CS complex. More recently, Faure et al. (1996; 1997) studied the properties of dimyristoylphosphatidylcholine-cholesterol sulfate (DMPC-CS) membranes, using microscopy, x-ray diffraction, and NMR techniques. They observed that CS has a smaller ordering effect on acyl tails compared to CH and can bind more water molecules. It was proposed that changes in the lipid headgroup conformations and positioning of CS molecules in the membrane may be responsible for the observed behavior. However, no direct experimental evidence that would support this hypothesis exists at the present time. More information about the properties of phospholipid membranes in the presence of CS on the molecular level can be obtained by using computer simulation techniques. To study the changes in membranes when CH is replaced by CS we performed a molecular dynamics simulation of a dipalmitoylphosphatidylcholine-cholesterol sulfate (DPPC-CS) membrane at a 1:1 ratio on a nanosecond time scale. The data from these simulations were compared to the data from our previous simulations on pure DPPC (Smondyrev and Berkowitz, 1999c) and DPPC-CH (Smondyrev and Berkowitz, 1999b) membranes.

METHODS

We report the results of a molecular dynamics simulation of a model bilayer made of DPPC and CS in water. We used the united atom force

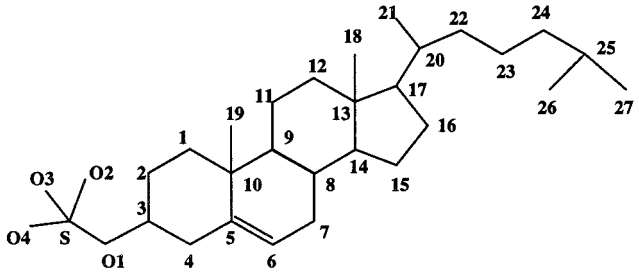

FIGURE 1 Structure of a cholesterol sulfate molecule. Carbon atoms are labeled with numbers; hydrogens are not shown.

field for DPPC molecules employed in our recent simulations of the DPPC-H_2O system (Smondyrev and Berkowitz, 1999c). Parameters for the CS molecules were taken from the united atom AMBER force field (Weiner et al., 1984) and were identical, except for the sulfate group, to the set of parameters used for cholesterol in our recent simulations of the DPPC-CH-H_2O system (Smondyrev and Berkowitz, 1999b). Force field parameters for the sulfate group were adapted with some modifications from Huige and Altona (1995). Partial atomic charges of CS (see Table 1) were calculated using the Gaussian 98 program at the 6–31G(d) basis set level and the Mulliken population analysis (Frisch et al., 1998). We employed the TIP3P water model (Jorgensen et al., 1983) in our simulation. Our system consists of 32 DPPC, 32 CS (lipid:sterol ratio of 1:1), and 1312 water molecules. Because CS molecules have a total charge of -1, we added 32 sodium ions (Na^+) to ensure the electroneutrality of the system.

Initial equilibration involved several steps and was similar to the procedure employed in the preparation of the DPPC-CH-water system (Smondyrev and Berkowitz, 1999b). First, we created a monolayer containing 16 DPPC and 16 CS molecules. Coordinates of DPPC molecules were obtained by adding two carbon atoms to each tail of the DMPC molecule, coordinates of which were determined by Vanderkooi (1991). Coordinates of CS molecules were determined by taking coordinates of the CH molecule for the crystal structure (Shieh et al., 1981) and replacing the hydroxyl group (*OH*) with a sulfate group (SO_4^-). DPPC and CS molecules were then arranged in the plane of the membrane such that CS molecules alternated with lipid molecules (see Fig. 2), as in structure A of the DPPC-CH membrane (Vanderkooi, 1994; Smondyrev and Berkowitz, 1999b). This particular arrangement was selected to reduce electrostatic repulsion between negatively charged CS molecules. Thus regular distribution of sterol molecules was preferred to the arrangement with lipid and sterol domains as in structure B of the DPPC-CH membrane (Vanderkooi, 1994; Smondyrev and Berkowitz, 1999b). The initial area per DPPC-CS heterodimer was 100 $Å^2$, as in simulations of DPPC-CH membranes at

TABLE 1 Partial atomic charges for a cholesterol sulfate molecule

Atom	Charge	Atom	Charge	Atom	Charge
C1	−0.029	C12	0.009	C23	0.001
C2	0.070	C13	−0.071	C24	0.010
C3	0.312	C14	−0.006	C25	−0.018
C4	0.074	C15	0.010	C26	0.000
C5	0.047	C16	−0.016	C27	0.000
C6	−0.099	C17	0.015	S1	1.718
C7	−0.002	C18	0.018	O1	−0.747
C8	−0.002	C19	0.034	O2	−0.753
C9	0.001	C20	−0.014	O3	−0.753
C10	−0.074	C21	0.000	O4	−0.753
C11	0.010	C22	0.008		

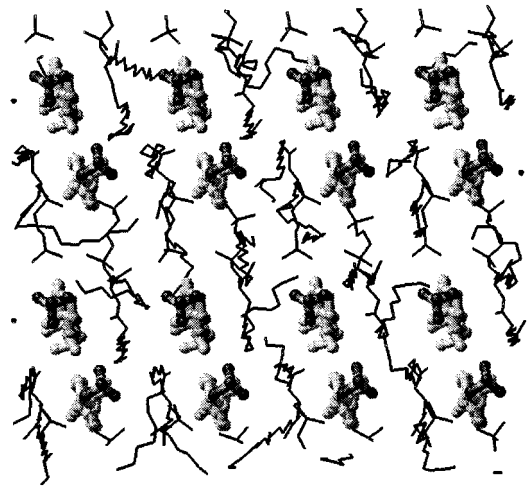

FIGURE 2 Initial structure of the DPPC:CS membrane. DPPC molecules are shown as black wires, and cholesterol sulfate molecules as ball and stick. Water molecules were removed for clarity.

lipid:sterol ratios of 1:1. Sodium atoms were placed at a distance of ~6 Å (which corresponds to approximately two layers of water molecules) above the sulfate group of CS molecules. This monolayer was then equilibrated for 20 ps with phosphorus atoms of DPPC, with all CS atoms and sodium counterions held fixed. The final configuration of the monolayer was used to construct a bilayer, using the P_2 symmetry group and adjusting the distance between phosphorus atoms in the two halves of bilayer to 44 Å. The bilayer was equilibrated for another 20 ps with the same constraints. After that 1312 water molecules were added, and the lamellar spacing was gradually decreased to 66 Å, allowing the system to equilibrate for 2 ps at each step. At this stage counterions were allowed to move while phosphorus atoms of DPPC and CS atoms were constrained as before. After adjusting the dimensions of the simulation cell, we performed a 50-ps constant-volume simulation, allowing all atoms of DPPC molecules to move freely. The CS ring system was still constrained while the sulfate group and sterol tail were unconstrained. After this step we increased the temperature of the system and then reduced it in a series of 20-ps simulations (T = 423, 393, 363, 343, 333, and 323 K). This step introduced disorder into the DPPC and CS tails. Finally, all constraints were removed, and the system was equilibrated for 100 ps at constant volume and temperature (T = 323 K).

After equilibrating the system, we carried out a 1400-ps molecular dynamics simulation at constant pressure (P = 0 atm) and temperature (T = 323 K) with periodic boundary conditions. Dimensions of the simulation cell were controlled with a Hoover barostat, with thermostat and barostat relaxation times of 0.2 ps and 0.5 ps, respectively. All bonds were constrained using the SHAKE algorithm, with a tolerance of 10^{-4}. The integration time step was 0.002 ps. Columbic interactions were calculated using the Ewald summation technique, with a tolerance of 10^{-4}. The real space part of the Ewald sum and van der Waals interactions were truncated at 10 Å. Calculations were performed on a Cray-T3E at the Texas Advanced Computing Center, using the DL_POLY simulation package (version 2.8, developed at Daresbury Laboratory, England) (Smith and Forester, 1996).

RESULTS

In Fig. 3 we show the average area of DPPC-CS heterodimers as a function of time and compare it with the results obtained in simulations of DPPC-CH bilayers at a

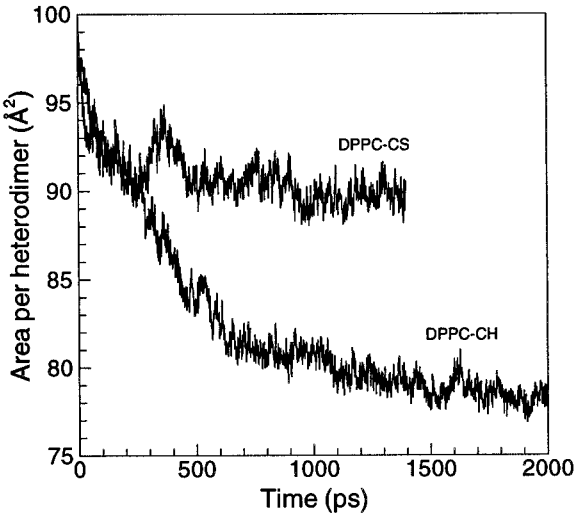

FIGURE 3 Areas per DPPC-CS heterodimer (*top curve*) and DPPC-CH heterodimer (50 mol% sterol, structure A; *bottom curve*) as a function of time.

lipid:sterol ratio of 1:1. After ~500 ps the area of the DPPC-CS heterodimer converged to a plateau value of 90.1 ± 0.8 Å^2. As we can see, the relaxation of the heterodimer area to its equilibrium value is much faster in the DPPC-CS bilayer compared to the case of the DPPC-CH bilayer. The average value of the DPPC-CS heterodimer area is larger than the area of the DPPC-CH heterodimer (78.5 Å^2 in structure A). Replacement of a small hydroxyl group in CH by a bulky, charged sulfate group in CS affects the packing of lipid and sterol molecules in the lipid membrane as well as the positioning of CS with respect to bilayer center.

In Fig. 4 we plot the electron density profiles for the pure DPPC, DPPC-CH, and DPPC-CS bilayers. The peak-to-peak distance for bilayers with CS (37.2 Å) is somewhat intermediate between corresponding values for pure DPPC (36 Å) and DPPC-CH (41.2 Å at 50% sterol) bilayers. The shape of the electron density profile for the DPPC-CS bilayer has features similar to the ones observed in the pure DPPC bilayer.

In Table 2 we show the average distances from the bilayer center to different atoms in DPPC, CH, and CS molecules. The distance from the bilayer center to phosphorus atoms in the DPPC-CS membrane is intermediate between distances for pure DPPC and DPPC-CH bilayers, which is in agreement with electron density profiles (see Fig. 4). Distances to DPPC carbon atoms in the DPPC-CS bilayer are again intermediate between corresponding values obtained for DPPC and DPPC-CH membranes, but the distances to carbon atoms in sterol rings are quite similar for DPPC-CH and DPPC-CS bilayers. By comparing distances to carbon atoms in DPPC tails in all three systems we can conclude that the length of the hydrocarbon tails is increasing from DPPC to DPPC-CS and reaches its maximum in the DPPC-CH bilayer. Orientation of sterol molecules is adjusting to match the DPPC hydrophobic thickness and is characterized by the angle between the vector connecting the C_3 and C_{17} atoms in sterol rings and the normal to the bilayer. In the DPPC-CS bilayer this angle is 19 ± 1°, which is larger than the angle determined for the DPPC-CH bilayer (11 ± 1°) and is comparable to the tilt angle found in the DPPC-CH bilayer at a DPPC:CH ratio of 8:1 (20 ± 3°). To determine the positions of CS sulfate groups we plotted distributions of several DPPC and CS atoms and compared them with distributions obtained for DPPC-CH-water systems (see Fig. 5). We can see that the peak of the sulfur distribution is located only slightly below the peak of the DPPC phosphorus distribution and above the peak of

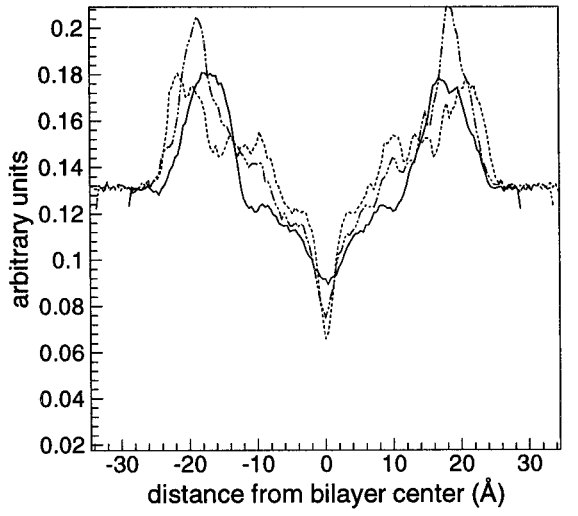

FIGURE 4 Electron density profiles for pure DPPC (——), DPPC-CH (– – –) and DPPC-CS (– · · –) membranes.

TABLE 2 Average distances (in Å) from the bilayer center to atoms in DPPC, CH, and CS molecules for pure DPPC, DPPC-CH (50 mol% sterol, structure A), and DPPC-CS membranes

Atoms	DPPC	DPPC-CH	DPPC-CS
DPPC			
P	19.0 ± 2.0	22.1 ± 1.2	20.5 ± 1.7
C_γ	19.5 ± 3.6	23.4 ± 2.4	21.0 ± 3.4
C_α	19.5 ± 2.5	22.8 ± 2.0	20.9 ± 2.5
C_β	19.4 ± 2.9	22.7 ± 1.7	21.1 ± 2.2
C_{G3}	17.2 ± 2.0	20.2 ± 1.4	18.8 ± 1.8
C_4	11.7 ± 1.9	14.8 ± 1.3	12.8 ± 1.7
C_5	10.8 ± 1.9	13.6 ± 1.4	11.8 ± 1.7
C_9	7.1 ± 1.9	8.9 ± 1.4	7.6 ± 1.7
C_{14}	3.2 ± 1.7	3.2 ± 1.8	2.6 ± 1.5
C_{15}	2.1 ± 2.4	2.3 ± 2.2	1.6 ± 2.0
Sterol			
C_3		16.6 ± 0.2	16.6 ± 0.2
C_{17}		8.2 ± 0.2	8.5 ± 0.2
C_{27}		1.8 ± 0.2	2.7 ± 0.2

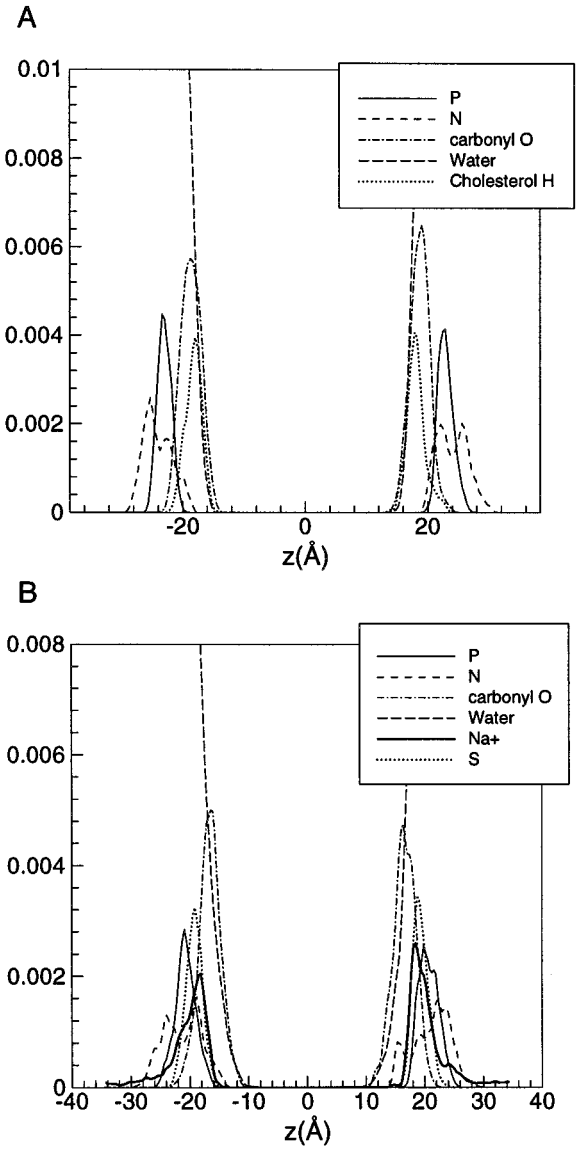

FIGURE 5 Distribution of atom densities (in atom/Å^3) along the bilayer normal for DPPC-CH (*A*) and DPPC-CS (*B*) membranes.

DPPC carbonyl oxygens. In membranes with cholesterol, peaks corresponding to CH hydroxyl groups and DPPC carbonyl oxygens were at approximately the same distance from the bilayer center. Water can still penetrate up to the carbonyl group in the DPPC-CS membrane. The distribution of sodium counterions peaks at approximately the same distance from the bilayer center as the sulfur distribution and decays slowly toward the water layer. In Fig. 6 we plotted *S*-Na^+ and *P*-Na^+ radial distribution functions. The first peak of the *S*-Na^+ distribution function, located at 3.2 Å, indicates that sodium ions are close to the sulfate group and therefore have a high tendency to interact with this group. The second peak of the *S*-Na^+ rdf (located at 3.7 Å) coincides with the first peak of the *P*-Na^+ rdf. This feature

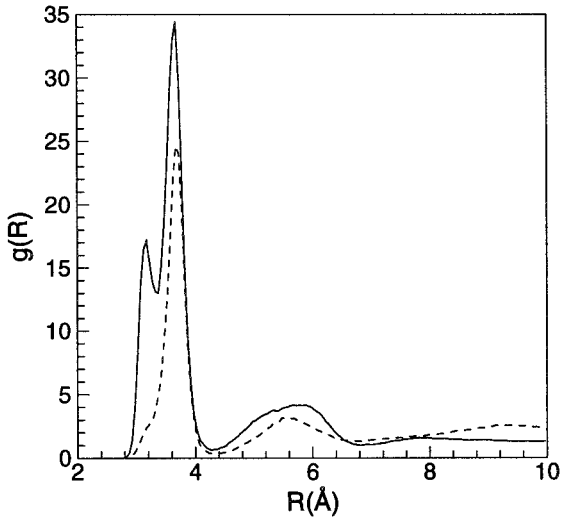

FIGURE 6 Pair distribution functions between the CS sulfur atom and Na^+ (——) and between DPPC phosphorus and Na^+ (– – –).

indicates that sodium ions form a "bridge" between negatively charged sulfate and phosphate groups.

The hydration of membrane containing DMPC and CS molecules was studied by Faure et al. (1996) and compared to membranes with CH. The authors presented two possible mechanisms that can explain changes in membrane hydration: 1) substitution of CH with CS in membrane changes the hydration of lipid molecules and 2) CS hydration is increased compared to CH. To test these hypotheses we calculated the average number of hydrogen bonds formed between water and DPPC, CH, and CS molecules. We defined the hydrogen bond, using the following criteria (Pasenkiewicz-Gierula et al., 1997): the distance between water and the DPPC (or sterol) oxygen is shorter than 3.25 Å, and the angle between the vector linking DPPC (or sterol) oxygen with water oxygen and H-O bond of the water is less than 35°, as proposed by Raghavan et al. (1992). In Table 3 we show the average number of hydrogen bonds formed with different oxygen atoms in DPPC molecules. The total numbers of hydrogen bonds per DPPC molecule are very close for DPPC and DPPC-CH membranes. When CH is replaced with CS the total number of hydrogen bonds becomes ~20% smaller. The changes in

TABLE 3 Average number of hydrogen bonds per DPPC molecule formed between water and different DPPC oxygens

	DPPC	DPPC-CH	DPPC-CS
O_{12}	0.53	0.55	0.53
O_{11}	0.22	0.26	0.21
O_{14}	1.67	1.73	1.52
O_{13}	1.70	1.63	1.31
O_{22}	1.38	1.46	0.80
O_{32}	0.54	0.52	0.48
Total	6.04	6.15	4.85

the number of hydrogen bonds are more pronounced for oxygen atoms located closer to the bilayer center. With respect to the number of hydrogen bonds between sterol molecules and water, we calculate that in DPPC-CH membranes CH forms only ~0.9 hydrogen bonds with water molecules, while the average number of hydrogen bonds between CS and water is 4.3 and is comparable with the average number of hydrogen bonds per DPPC molecule in the DPPC-CS bilayer (see Table 3). This result is not surprising because water binding sites on the CS sulfate group are similar to the ones on the DPPC phosphate group. The sulfate group is located only slightly below the DPPC phosphate group and is easily accessible to water molecules. Thus we conclude that two possible mechanisms suggested by Faure et al. are indeed correct.

Faure and Dufourc (1997) suggested that changes in the lipid hydration level in membranes containing CS may be due to reorientation of the lipid headgroup. Scherer and Seelig (1989) showed that surface electric charges influence the orientation of the palmitoyloleoylphosphatidylcholine polar headgroup. When the charge at the membrane surface is negative, the positively charged end of the choline group moves toward the membrane interior because of electrostatic attraction. The orientation of the headgroup is characterized by the angle (θ) between the vector connecting phosphorus and nitrogen atoms in a DPPC headgroup and the bilayer normal. The average values of this angle are similar in pure DPPC ($\theta \simeq 81°$) and DPPC-CS ($\theta \simeq 82°$) membranes. In DPPC-CH membranes the nitrogen end of the P-N dipole moves toward the water layer, and the average angle, $\theta \simeq 72°$ (50 mol% sterol, structure A), becomes smaller. Distributions of cos θ (see Fig. 7) also reflect the tendency of the P-N vector to reorient toward the bilayer center. General features of the cos θ distribution for the DPPC-CS bilayer are similar to the one for a pure DPPC bilayer, except for the regions where cos $\theta \approx \pm 1$, where the distribution for the DPPC-CS membrane is more highly populated. We propose that the tendency of the P-N vector to point toward the bilayer center is due to the interaction between positively charged choline and negatively charged sulfate groups. In Fig. 8 we show the S-N and S-P radial distribution functions for the DPPC-CS bilayer. While the first peak in the S-P distribution is broad, the peak of the S-N distribution is more distinct. Positions of the peaks indicate that because of electrostatic attraction the average distance between choline and sulfate groups is less than the distance between phosphate and sulfate groups. As we have mentioned already, the replacement of CH by CS changes the hydration of lipid molecules, and the hydration of CS is increased compared to CH. However, it is not clear whether the reduction in the number of hydrogen bonds between DPPC and water molecules in the DPPC-CS bilayer compared to DPPC and the DPPC-CH bilayer is due to the reorientation of the headgroup. It is also possible that water interacts more strongly with a sulfate group than with DPPC carbonyl oxygens, which results in the observed reduction in the number of hydrogen bonds.

Faure et al. (1996) also performed comparative studies of the effects of CH and CS on the first spectral momentum M_1 and the Sn-2 chain order parameter in DMPC membranes with 30 mol% sterol. The average value of the S_{CD} order parameter in the plateau region is smaller for the DPPC-CS bilayer than the corresponding value for the DPPC-CH bilayer, which indicates that the ordering effect of CS is less than that of CH. We calculated the deuterium order parameter, S_{CD}, using the following expression:

$$-S_{CD} = 2/3\ S_{xx} + 1/3\ S_{yy} \quad (1)$$

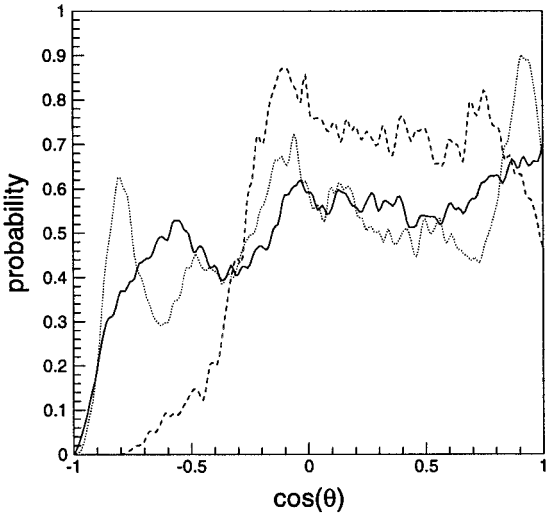

FIGURE 7 Distributions of the cosine of the angle between the P-N vector and the bilayer normal in pure DPPC (——), DPPC-CH (– – –), and DPPC-CS (· · · · ·) membranes. When cos θ is positive, the P-N vector points into the water layer.

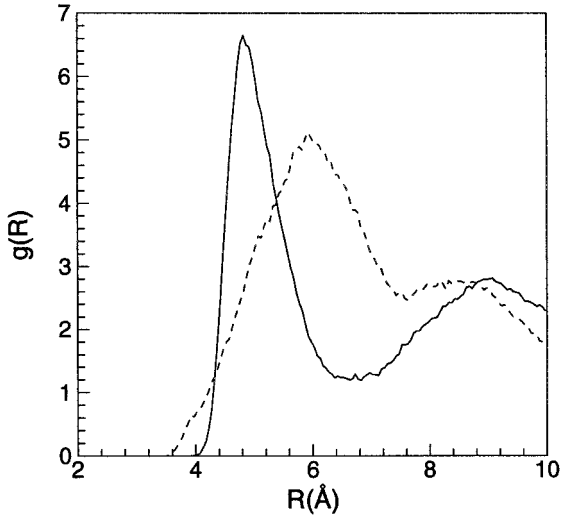

FIGURE 8 Pair distribution functions between the CS sulfur atom and DPPC atoms. ——, S-N; – – –, S-P.

where $S_{ij} = \langle 1.5 \cos \theta_i \cos \theta_j - 0.5\delta_{ij} \rangle$; θ_i is the angle between the ith molecular axis and the bilayer normal (z axis). (For more details see Egberts and Berendsen (1988).) In Fig. 9 we compare $-S_{CD}$ values for the Sn-2 chain from our simulations of DPPC (Smondyrev and Berkowitz, 1999c), DPPC-CH (50 mol% sterol, structure A) (Smondyrev and Berkowitz, 1999b), and DPPC-CS membranes. Incorporation of CS into the lipid bilayer increases the order in DPPC acyl chains, but to a lesser degree than does CH. The average hydrocarbon chain order, which is defined through the average order parameter $\langle -2S_{CD} \rangle$ (the average is taken over all carbon atoms in the lipid tails), has the lowest value for the DPPC bilayer ($\langle -2S_{CD} \rangle \simeq 0.34$), increases to ($\langle -2S_{CD} \rangle \simeq 0.50$) for the DPPC-CS bilayer, and is at maximum in the DPPC-CH bilayer ($\langle -2S_{CD} \rangle \simeq 0.72$). A similar trend is observed for the average number of *gauche* defects. As the acyl chain order rises from DPPC to DPPC-CS and to DPPC-CH, the average number of *gauche* defects per lipid tails decreases: from 3.50 for DPPC to 3.30 for DPPC-CS and to 2.55 for DPPC-CH (structure A). The average acyl chain length is another characteristic of the tail ordering. Again, the values obtained in the simulation of DPPC-CS membrane are intermediate between values for DPPC and DPPC-CH membranes (see Table 4). Interestingly, Sn-1 and Sn-2 tail lengths are slightly different for DPPC-CS membrane (Sn-2 tails are slightly longer than those of Sn-1) but follow the trend observed in the DPPC-CH bilayer at 50 mol% sterol (structure A).

Replacement of CH with CS in the lipid bilayer also results in dramatic changes in dipole potential $\psi(z)$ across the bilayer:

$$\psi(z) - \psi(0) = -\int_0^z dz' \int_0^{z'} \rho(z'')dz'' \qquad (2)$$

TABLE 4 Hydrocarbon chain lengths (Å) in DPPC, DPPC-CS, and DPPC-CH membranes

	DPPC	DPPC-CS	DPPC-CH
Sn-1	13.6	14.0	15.3
Sn-2	13.4	14.9	16.1

where $\rho(z)$ is the local excess charge density. In Fig. 10 we show the total potential for DPPC, DPPC-CS, and DPPC-CH bilayers. The total potentials for DPPC-CS and DPPC-CH membranes have opposite signs. In addition, the absolute value of this potential for DPPC-CS ($-200\ mV$) is smaller than the value obtained for the DPPC-CH system ($+1000\ mV$).

To understand the relationship between the bilayer structure and the dipole potential we also plotted separate contributions to the electrostatic potential due to water, DPPC Sn-1 and Sn-2 ester groups, lipid headgroups, and sterol molecules (see Fig. 11). The contribution of water is positive for all three systems. Dipole potentials due to DPPC headgroups and ester groups are ~30% greater for DPPC membrane than for DPPC:CS membrane. This is more than fully accounted for by the fact that the average area per DPPC is ~62 Å^2 and the average area per DPPC:CS dimer is ~90 Å^2. The contributions to the dipole potential due to DPPC headgroups and two ester groups become markedly different for DPPC:CH membranes. The ester groups are directed less toward the water phase in the DPPC:CH membrane, thus reducing their electrostatic potential. This may be a manifestation of either the interaction between the DPPC carbonyl groups and the cholesterol hydroxyl group or the condensing effect of cholesterol. The dipole potential due to DPPC headgroups becomes larger in the DPPC:CH

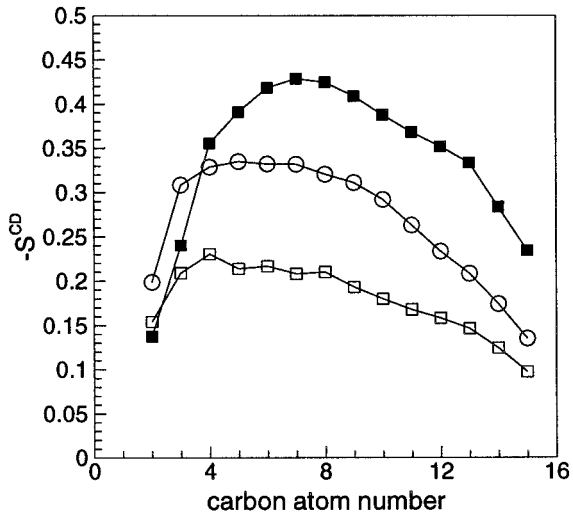

FIGURE 9 Deuterium order parameter—S_{CD} in DPPC Sn-2 tails for pure DPPC (□), DPPC-CS (○), and DPPC-CH (■) membranes.

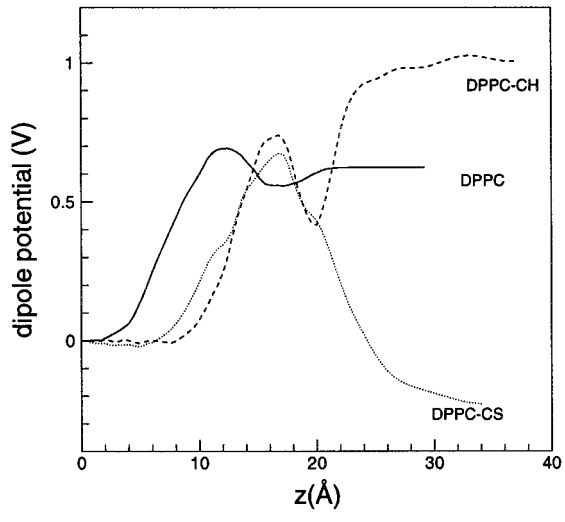

FIGURE 10 Dipole potential for pure DPPC (——), DPPC-CH (– – –), and DPPC-CS (· · · · ·) membranes. $Z = 0$ corresponds to the middle of the water layer.

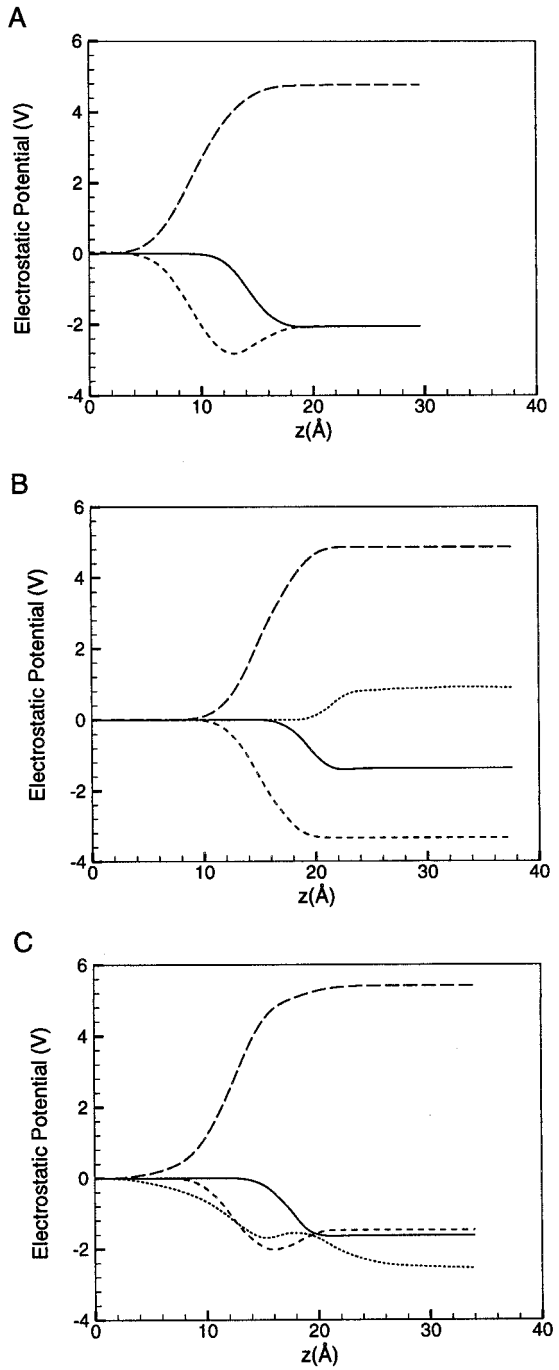

FIGURE 11 Separate contributions to the electrostatic potential of the DPPC (*A*), DPPC:CH (*B*), and DPPC:CS (*C*) membranes due to water (*long dashed lines*), DPPC headgroups (*short dashed lines*), DPPC ester groups (*solid lines*), and cholesterol (or cholesterol sulfate) (*dotted lines*).

bilayer, which reflects the higher tendency of the P-N vector to orient toward the water layer. The dipole potential profile due to lipid headgroups in the DPPC:CH bilayer is monotonic, which suggests that the pronounced minima, observed for DPPC and DPPC:CS systems, were due to the headgroups with the P-N vector directed toward the bilayer center. This can also be seen from the distributions of the angle between the P-N vector and bilayer normal (see Fig. 7).

To explain the differences in the effects of CH and CS on the dipole potential we can employ a capacitor model (Schweighofer et al., 1997). The DPPC phosphate group has a negative (-1) charge and on average is located closer to the bilayer center than the positively ($+1$) charged choline group. The contribution of the DPPC headgroup to the dipole potential is negative (Smondyrev and Berkowitz, 1999a), and we can expect that CS contributes to the dipole potential similarly. The sulfate group has a negative charge (-1), while sodium ions are positively charged and play the role of a second plate of the capacitor. We can see from Fig. 5 that counterions are located farther from the bilayer center than is the sulfate group. As a result, the CS contribution to the dipole potential is negative. Contrary to CS, the CH contribution to the dipole potential is positive. The CH hydroxyl group (OH) is negatively charged and is located farther from the bilayer center than is the positively charged C_3 carbon. These two charges make the major contribution to the portion of the dipole potential due to CH. Thus the effect of the capacitor due to CH is the opposite of the effect of CS. We can expect that with varying relative concentrations of CH and CS in the membrane, the total dipole potential will change from a large positive value for DPPC-CH to a negative value for DPPC-CS membranes; and, for some CH-CS ratio, the total dipole potential can become zero.

CONCLUSIONS

We performed comparative studies of DPPC-CH and DPPC-CS membranes at 50 mol% concentrations of sterol. We found that incorporation of CS in lipid membranes results in a condensing effect, although this effect is not as strong as in DPPC-CH membranes at the same lipid:sterol ratios. This is also evident from examination of deuterium order parameter profiles and measurement of hydrocarbon chain lengths. DPPC tails are more disordered in DPPC-CS compared to DPPC-CH membranes. The lengths of DPPC tails are greater in membranes containing CH compared with those with CS. These results are in good agreement with the experimental data of Faure et al. (1996), who concluded that membranes containing CH are thicker than those containing CS. Because of hydrophobic mismatch, CS molecules exhibit a larger tilt with respect to the bilayer normal compared to CH. Faure et al. (1996) also suggested that there is no large difference in the vertical locations of the two steroids and that CS with its bulky hydrated sulfate group acts as a spacer. Results of our simulations support this model. We found that C_3 carbon atoms in sterol rings of CH and CS are located at approximately the same distance from the bilayer center. Bulky sulfate groups are placed only slightly below the lipid phosphate groups, which may be the dominant factor in the observed increase of the area

per lipid-sterol dimer. As a consequence, lipid tails do not interact with CS rings as strongly as with CH and become more disordered.

Experimental data also indicate that CS-containing membranes become more hydrated (Faure et al., 1996). Faure et al. proposed that the P-N dipole of DPPC moves away from the water layer because of the interaction between the lipid headgroup and the sulfate moiety. Phosphate and Sn-2 carbonyl groups bind fewer water molecules, and as a result lipid molecules are less hydrated in the presence of CS than in the presence of CH. Furthermore, the differences in hydration of CH- and CS-containing membranes can be attributed to a greater hydration of CS. Results of our simulations indicate that this picture is correct: the P-N dipole is indeed oriented more parallel to the membrane surface when CH is replaced with CS. We found that the average numbers of hydrogen bonds formed between water molecules and DPPC oxygens are very similar for DPPC and DPPC-CH membranes, but decrease for the DPPC-CS membrane. As evident from Table 3, this decrease is due primarily to the dehydration of three water-binding sites: O_{13} and O_{14} in the phosphate group and the Sn-2 carbonyl group. It should be noted that all three sites are located close to the sulfate groups, which suggests that specific interactions with CS may be responsible for the dehydration of lipid molecules. We did not find a noticeable difference in hydrogen bonding of the Sn-1 carbonyl group, which is consistent with the experimental results of Chiou et al. (1992).

The dipole potential for the DPPC-CS membrane changes its sign compared to DPPC-CH membrane, and the contribution of CS molecules is opposite to that due to CH. The change in the sign of the dipole potential was also found in simulations of membrane containing $DPPS^{-}$ with Na^{+} counterions and water (Cascales et al., 1996). The absolute value of the total dipole potential calculated in that simulation is ~ 2 V, which is 10 times larger than the value obtained in our work. Although it is not possible to make a direct quantitative comparison between the results obtained in the present work and data of Cascales et al. (1996), because of the different parametrizations, the qualitative agreement between the two simulations is rather good. We predict that for a membrane consisting of DPPC, CH, and CS molecules the dipole potential would vanish at some CH:CS ratio. According to Cevc and Marsh (1985), the hydration force is proportional to the square of the electrostatic potential, and therefore it would be minimal in this situation. We also found that in membranes containing CS, DPPC headgroups orient more parallel to the bilayer center than in DPPC:CH membranes. As a result of the interactions between the lipid's choline groups and CS sulfate groups, membrane rigidity increases, which may at least partially explain why CS-containing membranes are more stable and less fusogenic. These results resemble our recent findings for the DPPC:dimethyl sulfoxide system (Smondyrev and Berkowitz, 1999a), from which we have concluded that these factors may reduce repulsion when two membranes are brought close together. We propose that the same factors may also promote the adhesion of two CS-containing membranes. At the present time we are not aware of any experiments on membranes containing cholesterol sulfate in which electrostatic potential or hydration forces were measured. Such measurements could determine whether there is a relationship between the value of the dipole potential and hydration forces and provide evidence supporting our predictions.

Calculations were performed on a Cray-T3E at the Texas Advanced Computing Center. Computational support from the National Partnership for Advanced Computing Infrastructure is gratefully acknowledged. We are grateful to reviewers for their constructive criticism of the manuscript.

The studies reported in this work were supported by the National Science Foundation under grant MCB9604585.

REFERENCES

Bleau, G., G. Lalumiere, A. Chapdelaine, and K. Roberts. 1975. Red cell surface structure stabilization by cholesterol sulfate as evidenced by scanning electron microscopy. *Biochim. Biophys. Acta.* 375:220–223.

Cascales, J. J. L., H. J. C. Berendsen, and J. G. de la Torre. 1996. Molecular dynamics simulation of water between two charged layers of dipalmitoylphosphatidylserine. *J. Phys. Chem.* 100:8621–8627.

Cevc, G., and D. Marsh. 1985. Hydration of noncharged lipid bilayer membranes. Theory and experiments with phosphatidylethanolamines. *Biophys. J.* 47:21–31.

Cheetham, J. J., R. M. Epand, M. Andrews, and T. D. Flanagan. 1990. Cholesterol sulfate inhibits the fusion of Sendai virus to biological and model membranes. *J. Biol. Chem.* 265:12404–12409.

Chiou, J. S., P. R. Krishna, H. Kamaya, and I. Ueda. 1992. Alcohols dehydrate lipid membranes: an infrared study on hydrogen bonding. *Biochim. Biophys. Acta.* 1110:225–233.

Egberts, E., and H. J. C. Berendsen. 1988. Molecular-dynamics simulation of a smectic liquid crystal with atomic detail. *J. Chem. Phys.* 89: 3718–3732.

Elias, P. M., M. L. Williams, M. E. Maloney, J. A. Bonifas, B. E. Brown, S. Grayson, and E. H. Epstein. 1984. Stratum-corneum lipids in disorders of cornification—steroid sulfatase and cholesterol sulfate in normal disquamation and the pathogenesis of recessive x-linked ichthyosis. *J. Clin. Invest.* 74:1414–1421.

Faure, C., and E. J. Dufourc. 1997. The thickness of cholesterol sulfate-containing membranes depends upon hydration. *Biochim. Biophys. Acta.* 1330:248–252.

Faure, C., J. F. Tranchant, and E. J. Dufourc. 1996. Comparative effects of cholesterol and cholesterol sulfate on hydration and ordering of dimyristoylphosphatidylcholine membranes. *Biophys. J.* 70:1380–1390.

Fayrer-Hosken, R. A., B. G. Brackett, and J. Brown. 1987. Reversible inhibition of rabbit sperm-fertilizing ability by cholesterol sulfate. *Biol. Reprod.* 36:878–883.

Frisch, M. J., G. W. Trucks, H. B. Schlegel, G. E. Scuseria, M. A. Robb, J. R. Cheeseman, V. G. Zakrzewski, J. A. Montgomery, R. E. Stratmann, J. C. Burant, S. Dapprich, J. M. Millam, A. D. Daniels, K. N. Kudin, M. C. Strain, O. Farkas, J. Tomasi, V. Barone, M. Cossi, R. Cammi, B. Mennucci, C. Pomelli, C. Adamo, S. Clifford, J. Ochterski, G. A. Petersson, P. Y. Ayala, Q. Cui, K. Morokuma, D. K. Malick, A. D. Rabuck, K. Raghavachari, J. B. Foresman, J. Cioslowski, J. V. Ortiz, B. B. Stefanov, G. Liu, A. Liashenko, P. Piskorz, I. Komaromi, R. Gomperts, R. L. Martin, D. J. Fox, T. Keith, M. A. Al-Laham, C. Y. Peng, A. Nanayakkara, C. Gonzalez, M. Challacombe, P. M. W. Gill, B. G. Johnson, W. Chen, M. W. Wong, J. L. Andres, M. Head-Gordon,

E. S. Replogle, and J. A. Pople. 1998. Gaussian 98. Gaussian, Pittsburgh, PA.

Hanley, K., Y. Jiang, C. Katagiri, K. R. Feingold, and M. L. Williams. 1997. Epidermal steroid sulfatase and cholesterol sulfotransferase are regulated during late gestation in the fetal rat. *J. Invest. Dermatol.* 108:871–875.

Huige, C. J. M., and C. Altona. 1995. Force field parameters for sulfates and sulfanates based on ab initio calculations: extensions of AMBER and CHARMm fields. *J. Comp. Chem.* 16:56–79.

Jorgensen, W. L., J. Chandrasekhar, J. D. Madura, R. W. Impey, and M. L. Klein. 1983. Comparison of simple potential functions for simulating liquid water. *J. Chem. Phys.* 79:926–935.

Kagehara, M., M. Tachi, K. Harii, and M. Iwamori. 1994. Programmed expression of cholesterol sulfotransferase and transglutaminase during epidermal differentiation of murine skin development. *Biochim. Biophys. Acta.* 1215:183–189.

Kitson, N., M. Monck, K. Wong, J. Thewalt, and P. Cullis. 1992. The influence of cholesterol 3-sulphate on phase behaviour and hydrocarbon order in model membrane systems. *Biochim. Biophys. Acta.* 1111: 127–133.

Langlais, J., M. Zollinger, L. Plante, A. Chapdelaine, G. Bleau, and K. D. Roberts. 1976. Cholesterol sulfate and sterol sulfatase in the human reproductive tract. *Steroids.* 27:247–260.

Langlais, J., M. Zollinger, L. Plante, A. Chapdelaine, G. Bleau, and K. D. Roberts. 1981. Localization of cholesterol sulphate in human spermatozoa in support of hypothesis for the mechanism of capacitation. *Proc. Natl. Acad. Sci. USA.* 78:7266–7270.

McMullen, T. P. W., and R. N. McElhaney. 1996. Physical studies of cholesterol-phospholipid interactions. *Curr. Opin. Colloid Interface Sci.* 1:83–90.

Pasenkiewicz-Gierula, M., Y. Takaoka, H. Miyagawa, K. Kitamura, and A. Kusumi. 1997. Hydrogen bonding of water to phosphatidylcholine in the membrane as studied by a molecular dynamics simulation: location, geometry, and lipid-lipid bridging via hydrogen-bonded water. *J. Phys. Chem.* 101:3677–3691.

Raghavan, K., M. R. Reddy, and M. L. Berkowitz. 1992. A molecular-dynamics study of the structure and dynamics of water between dilaurophosphatidylethanolamine bilayers. *Langmuir.* 8:233–240.

Scherer, P. G., and J. Seelig. 1989. Electric charge effects on phospholipid headgroups. Phosphatidylcholine in mixtures with cationic and anionic amphiphiles. *Biochemistry.* 28:7720–7728.

Schweighofer, K. J., U. Essmann, and M. L. Berkowitz. 1997. Structure and dynamics of water in the presence of charged surfactant monolayers at the water/CCl_4 interface. A molecular dynamics study. *J. Phys. Chem. B.* 101:10775–10780.

Shieh, H. S., L. G. Hoard, and C. E. Nordman. 1981. The structure of cholesterol. *Acta Crystallogr. B.* 37:1538–1543.

Smith, W., and T. R. Forester. 1996. DL_POLY. Council for the Central Laboratory of the Research Councils, Daresbury Laboratory at Daresbury, Nr. Warrington, England.

Smondyrev, A. M., and M. L. Berkowitz. 1999a. Molecular dynamics simulation of DPPC bilayer in DMSO. *Biophys. J.* 76:2472–2478.

Smondyrev, A. M., and M. L. Berkowitz. 1999b. Structure of DPPC/cholesterol bilayer at low and high cholesterol concentrations: molecular dynamics simulation. *Biophys. J.* (in press).

Smondyrev, A. M., and M. L. Berkowitz. 1999c. United atom force field for phospholipid membranes. Constant pressure molecular dynamics simulation of DPPC/water system. *J. Comp. Chem.* 20:531–545.

Vanderkooi, G. 1991. Multibilayer structure of dimyristoylphosphatidylcholine dehydrate as determined by energy minimization. *Biochemistry.* 30:10760–10768.

Vanderkooi, G. 1994. Computation of mixed phosphatidylcholine-cholesterol bilayer structures by energy minimization. *Biophys. J.* 66: 1457–1468.

Weiner, S. J., P. A. Kollman, D. A. Case, U. C. Singh, C. Ghio, G. Alagonax, S. Profeta, and P. Weiner. 1984. A new force field for molecular mechanics simulation of nucleic acids and proteins. *J. Am. Chem. Soc.* 106:765–784.

Wells, R. S., and C. B. Kerr. 1966. The histology of ichthyosis. *J. Invest. Dermatol.* 46:530–535.